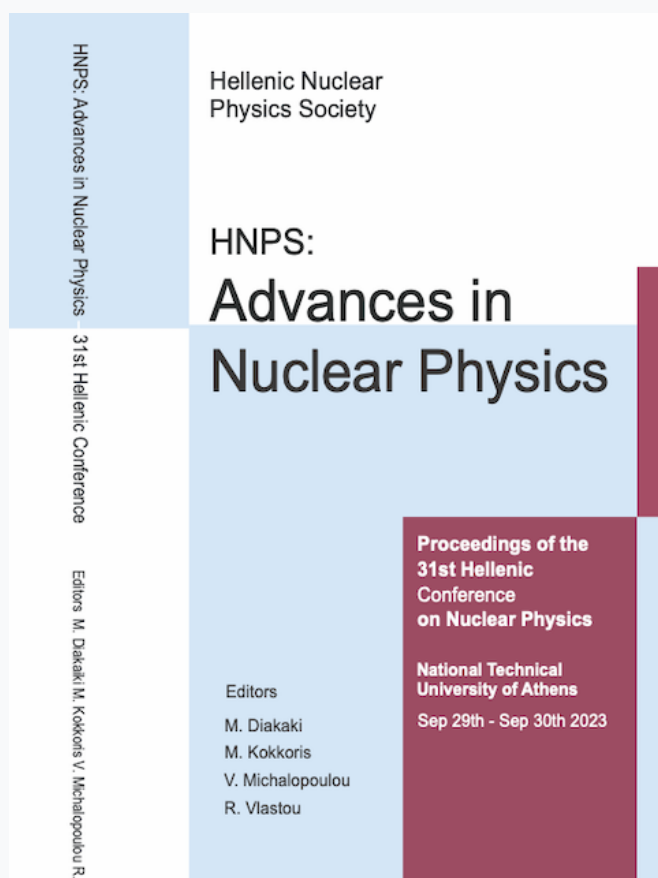


HNPS Advances in Nuclear Physics

Vol 30 (2024)

HNPS2023



Elastic scattering of $8B+90Zr$ at sub-barrier energies

K. Palli, A. Pakou, A. M. Moro, P. D. O'Malley, L. Acosta, A. Sántez-Bénitez, G. Souliotis, E. F. Aguilera, E. Andrade, D. Godos, O. Sgouros, V. Soukeras, C. Agodi, T. L. Bailey, D. W. Bardayan, C. Boomershine, M. Brodeur, F. Cappuzzello, S. Caramichael, M. Cavallaro, S. Dede, J. A. Dueñas, J. Henning, K. Lee, W. S. Porter, F. Rivero, W von Seeger

doi: [10.12681/hnpsanp.6120](https://doi.org/10.12681/hnpsanp.6120)

Copyright © 2024, K. Palli, A. Pakou, A. M. Moro, P. D. O'Malley, L. Acosta, A. Sántez-Bénitez, G. Souliotis, E. F. Aguilera, E. Andrade, D. Godos, O. Sgouros, V. Soukeras, C. Agodi, T. L. Bailey, D. W. Bardayan, C. Boomershine, M. Brodeur, F. Cappuzzello, S. Caramichael, M. Cavallaro, S. Dede, J. A. Dueñas, J. Henning, K. Lee, W. S. Porter, F. Rivero, W von Seeger

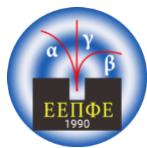


This work is licensed under a [Creative Commons Attribution-NonCommercial-NoDerivatives 4.0](https://creativecommons.org/licenses/by-nc-nd/4.0/).

To cite this article:

Palli, K., Pakou, A., Moro, A. M., O'Malley, P. D., Acosta, L., Sántez-Bénitez, A., Souliotis, G., Aguilera, E. F., Andrade, E., Godos, D., Sgouros, O., Soukeras, V., Agodi, C., Bailey, T. L., Bardayan, D. W., Boomershine, C., Brodeur, M., Cappuzzello, F., Caramichael, S., Cavallaro, M., Dede, S., Dueñas, J. A., Henning, J., Lee, K., Porter, W. S., Rivero, F., & von Seeger, W. (2024). Elastic scattering of $8B+90Zr$ at sub-barrier energies. *HNPS Advances in Nuclear Physics*, 30,

37-42. <https://doi.org/10.12681/hnpsanp.6120>



Elastic scattering of ${}^8\text{B}+{}^{90}\text{Zr}$ at 26.5 MeV

K. Palli^{1,2,*}, A. Pakou¹, A.M. Moro^{3,4}, P.D. O'Malley⁵, L. Acosta⁶, A. Sántez-Bénitez⁷,
G. Souliotis², E.F. Aguilera⁸, E. Andrade⁶, D. Godos⁶, O. Sgouros^{9,10}, V. Soukeras^{9,10},
C. Agodi⁹, T.L. Bailey⁵, D.W. Bardayan⁵, C. Boomers⁵, M. Brodeur⁵, F. Cappuzzello^{9,10},
S. Caramichael⁵, M. Cavallaro⁹, S. Dede^{5,11}, J.A. Dueñas¹², J. Henning⁵, K. Lee⁵, W.S. Porter⁵,
F. Rivero⁵, W. von Seeger⁵

¹ Department of Physics, The University of Ioannina, 45110 Ioannina, Greece

² Department of Chemistry, National and Kapodistrian University of Athens, 15771 Athens, Greece

³ Departamento de Física Atómica, Molecular y Nuclear, Universidad de Sevilla, Apartado 1065, E-41080 Sevilla, Spain

⁴ Instituto Interuniversitario Carlos I de Física Teórica y Computacional (iC1), Apartado. 1065, E-41080 Sevilla, Spain

⁵ Department of Physics and Astronomy, University of Notre Dame, Notre Dame, Indiana 46556, USA

⁶ Instituto de Física, Universidad Nacional Autónoma de México, A.P. 20-364, México City 01000, México

⁷ Departamento de Ciencias Integradas y Centro de Estudios Avanzados en Física, Matemáticas y Computación, Universidad de Huelva, 21071 Huelva, Spain

⁸ Departamento de Aceleradores y Estudio de Materiales, Instituto Nacional de Investigaciones Nucleares, Apartado Postal 18-1027, Código Postal 11801, Mexico City, Distrito Federal, Mexico

⁹ INFN Laboratori Nazionali del Sud, via Santa Sofia 62, 95125 Catania, Italy

¹⁰ Dipartimento di Fisica e Astronomia "Ettore Majorana", Università di Catania, via Santa Sofia 64, 95125 Catania, Italy

¹¹ Cyclotron Institute, Texas A&M University, College Station, Texas 77843, USA

¹² Centro de Estudios Avanzados en Física, Matemáticas y Computación, Universidad de Huelva, 21071 Huelva, Spain

Abstract Elastic scattering measurements for the reaction ${}^8\text{B}+{}^{90}\text{Zr}$ at the sub-barrier energy of 26.5 MeV (~ 0.9 VC.B.) were carried out in a recent experiment, realized at the *TriSol* radioactive beam facility of the University of Notre Dame. This experiment was performed in continuation of our previous work studying ${}^8\text{B}$ on the heavier target ${}^{208}\text{Pb}$, alongside with breakup measurements for the same reaction. The final goal is the determination of total reaction and breakup cross sections and the deduction of the direct to total cross section ratio. Preliminary experimental data for elastic scattering will be presented and compared with OMP and CDCC calculations.

Keywords Weakly-bound nuclei, elastic scattering, Coulomb barrier

INTRODUCTION

The investigation of reaction dynamics at near barrier energies for weakly bound stable or radioactive nuclei was pursued systematically the last 20 years [1-4]. It proved to be a fruitful play ground in relation with channel coupling effects affecting, either elastic scattering and probing a new type of the standard potential threshold anomaly [5], or/and the suppression and enhancement of fusion cross sections below and above barrier [1,3,6,7]. At deep sub-barrier energies and below the region that is well described by standard

* Corresponding author: konnapalli@chem.uoa.gr

coupled-channels theories, a fusion hindrance was established for heavy systems [8-10], affecting our concepts on astrophysical problems. In this respect, the reaction mechanisms and the competition between compound and direct processes at near and below barrier is of profound interest.

Searching for the reaction dynamics below barrier and in continuation of our previous work on ${}^8\text{B}+{}^{208}\text{Pb}$ at 30 MeV [11], we report here a similar study at the sub-barrier energy of 26.6 MeV for the system ${}^8\text{B} + {}^{90}\text{Zr}$. Our scientific motivation is related with a phenomenological prediction reported before in Ref. [12]. In this prediction, ratios of direct to total reaction cross sections were formed and mapped as a function of energy at below and above barrier energies, taking into account systematic results for fusion and total reaction cross section measurements for weakly bound nuclei. It was found that while at near-barrier energies this ratio is similar for all targets, and close to $\sim 20\%$, for energies below the barrier and for heavy targets this ratio increases up to $\sim 100\%$, leaving little or no room for fusion. For deep sub-barrier energies, it was already validated this prediction with our measurement on ${}^8\text{B}+{}^{208}\text{Pb}$ [11], where the dominance of breakup was reported at deep sub-barrier energies. In this work preliminary results on elastic scattering and breakup will be given for the same radioactive projectile, ${}^8\text{B}$ but on a medium mass target, ${}^{90}\text{Zr}$. The nucleus ${}^8\text{B}$ is an appealing nucleus with a proton halo and a binding energy of the proton to a ${}^7\text{Be}$ core of 0.137 MeV. Therefore, it is expected to present a large reaction cross section, possibly larger than the standard, and a large breakup cross section, allowing an easy measurement [12-14]. In the following, we will give some details of the experimental set-up and a preliminary analysis of our data. For elastic scattering Continuum Discretized Coupled Channel (CDCC) calculations and OMP calculations will be presented in comparison with the data. For breakup, we will describe our approach for discriminating ${}^7\text{Be}$ breakup fragments from the elastic scattered nuclei of the ${}^7\text{Be}$ beam, as part of a cocktail beam, used in this experiment. No breakup data will be presented at the moment.

EXPERIMENTAL DETAILS

The experimental part of this work was realised in August 2022 in the Nuclear Science Laboratory of the University of Notre Dame, employing the *TriSol* radioactive beam facility. Details about the operation of the facility can be found in [15]. The ${}^8\text{B}$ beam was produced in flight by the NSL 10 MV FN tandem accelerator. A ${}^6\text{Li}$ primary beam was accelerated at 37 MeV and impinged on a 2.5-cm-long gas target of ${}^3\text{He}$ at pressure of 850 Torr, producing a secondary cocktail beam of ${}^8\text{B}$ at 27.7 MeV, ${}^7\text{Be}$ at 20.1 MeV and ${}^7\text{Li}$ at 14.9 MeV. The products were then focused and guided by the three superconducting solenoids to a ${}^{\text{nat}}\text{Zr}$ target of 1.95 mg/cm² thickness. At the middle of the target, the beam energies correspond to 26.5 MeV, 19.2 MeV and 14.3 MeV for ${}^8\text{B}$, ${}^7\text{Be}$ and ${}^7\text{Li}$ respectively.

For the detector set-up, four two-stage ΔE -E telescopes were used. Each of these consisted of a DSSSD (Double-Sided Strip Silicon Detector) and a Pad silicon detector. Three of the telescopes were provided by the SIMAS (Sistema Móvil de Alta Segmentación) array of LEMA (Laboratorio Nacional de Espectrometría de Masas con Aceleradores) of the Physics Institute of the Autonomous National University of Mexico, and had DSSSDs with thickness of 20 μm , while the fourth one was provided by the Laboratorio de Interacciones Fundamentales (LIFE) of the research center of the Centro de Estudios Avanzados en Física, Matemáticas y Computación of the University of Huelva, Spain, with its DSSSD 15 μm thick. The silicon pad detectors were either 130 or 500 μm thick. The dimensions for the telescopes were 5.4 x 5.4 cm. Each DSSSD consists of 16 vertical and 16 horizontal strips providing the possibility for interstrip rejection and pixel-by-pixel analysis.

All four telescopes were positioned 59.9 mm from the target in symmetrical positions, covering an angular range of $\sim 20^\circ$ to 60° degrees in the forward direction and $\sim 110^\circ$ to 150° degrees in the backward direction.

ELASTIC SCATTERING ANALYSIS

The elastically scattered ^8B nuclei at the zirconium target were resolved in an excellent way from the other reaction products produced by boron or/and the other beams through the ΔE -E technique. A typical spectrum collected by a strip at 25° degrees is presented in Fig. 1.

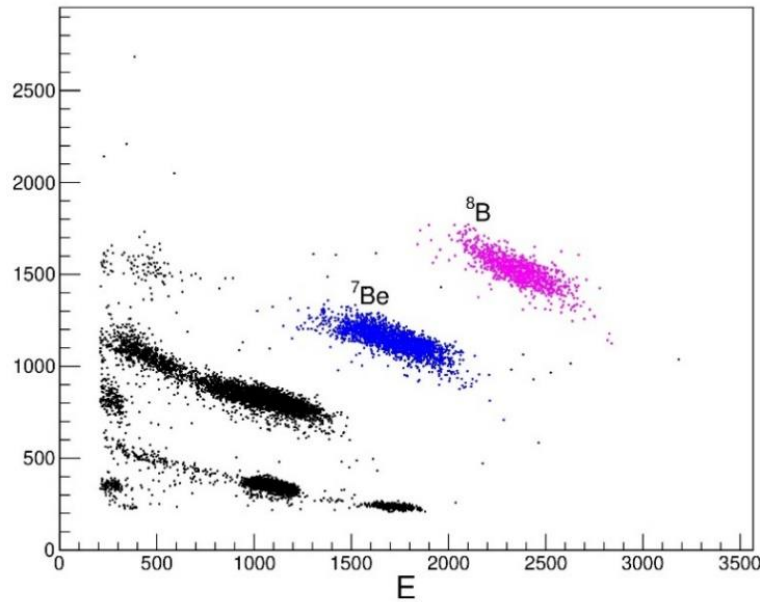


Figure 1. $\Delta E - E$ spectrum for $^8\text{B} + ^{90}\text{Zr}$ at $\sim 25^\circ$. ^8B nuclei are colored with pink and ^7Be with blue

Elastic scattering cross sections were deduced according to the following relation, employing the data for ^7Be at the energy of 20.6 MeV, simultaneously collected with the boron ones.

$$\frac{\sigma_{8B}(\theta)}{\sigma_{Ruth}^{8B}(\theta)} = \frac{N_{8B}(\theta)\sigma_{7Be}(\theta)}{N_{7Be}(\theta)\sigma_{Ruth}^{7Be}(\theta)} f \quad (1)$$

where $\sigma_{8B}(\theta)$ is the unknown differential cross section of ^8B elastically scattered at ^{90}Zr at an angle θ , σ_{7Be} is the ^7Be elastic scattering cross section at the same target, determined in a separate experiment [16,17] at an energy very close to the present one of the cocktail beam. The factor $f=F1/F2$ is the ratio of the beam fluxes in the two measurements and it was adjusted so that at forward angles the ratio of eq. (1) to be close to 1, due to Rutherford scattering. N_{8B} , N_{7Be} are the deduced yields of the elastically scattered ^8B and ^7Be nuclei respectively and σ_{Ruth}^{8B} , σ_{Ruth}^{7Be} are the Rutherford scattering cross sections for the two nuclei.

The results of the elastic scattering analysis, compared with CDCC and Optical Model calculations are presented in Fig. 2. The CDCC (Continuum Discretized Coupled Channel) calculation have been performed using a core (^7Be) + target interaction, by using the code FRESKO [18] while the Optical Model fits have been performed with the program ECIS by using the BDM3Y1 interaction [19]. CDCC calculations are in fair agreement with the data leading however to substantial differences with the OMP ones in the extracted

cross sections. The obtained cross sections are 380mb for the CDCC calculation and 180 ± 40 mb for the OMP fit. This disagreement between the data and the CDCC calculation requires further investigation.

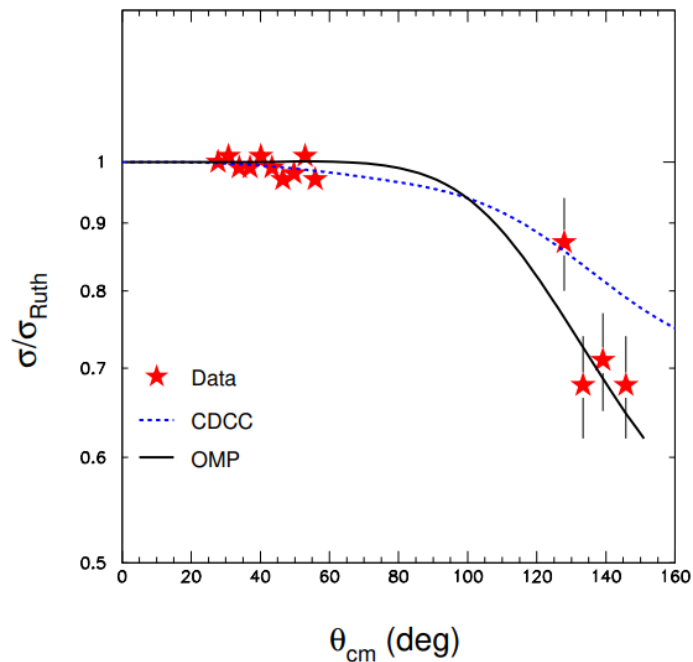


Figure 2. Differential elastic scattering cross sections over Rutherford cross sections as a function of the angle in the center of mass for the system $^8\text{B}+^{90}\text{Zr}$ at reaction energy 26.5 MeV. The experimental data are shown with the red stars and the dashed blue line and black line correspond to the CDCC and OMP calculations respectively.

BREAKUP ANALYSIS - CALIBRATION PROCESS

For our preliminary analysis of the break-up products, with goal the extraction of the direct-to-total reaction cross section ratio, it is imperative to be able to separate the elastically scattered ^7Be from the cocktail beam and the breakup products of the reaction. This can be achieved through the time-of-flight technique. For some of our data this separation was very good as it can be seen in Fig. 3. However, due to the inadequate separation of ^8B and ^7Be bands in the TOF spectra, for part of the data, it was found necessary to perform a detailed energy calibration of the DSSSDs with the goal to separate, the elastic ^7Be from the breakup products via energy.

For the calibration process, ^{228}Th was used as an alpha source, along with elastic scattering data from $^7\text{Be}+^{90}\text{Zr}$ at 28.2 MeV [16]. To calibrate the detectors appropriately, we must consider the non-uniformity in the thickness of the strips. Due to the very small thickness of the DSSSDs, we observed difference in the thickness throughout each strip. This difference in thickness corresponds to difference in the energy loss of the particles when passing through the ΔE part of the telescope for some of the strips. The effect can be observed in Fig. 4, as a splitting of the ΔE -E bands in the spectrum. To tackle this issue the calibration process had to be performed taking into account separately the top and bottom part of each strip, grouping together some of the n-strips accordingly. This process is currently in progress.

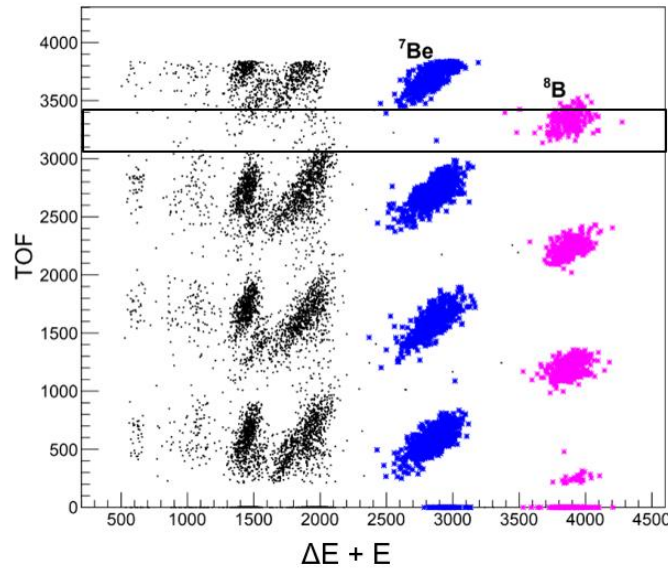


Figure 3. Time-of-flight spectrum as a function of the total energy. ^8B nuclei are colored with pink and ^7Be with blue. The black frame shows one of the time windows of ^8B .

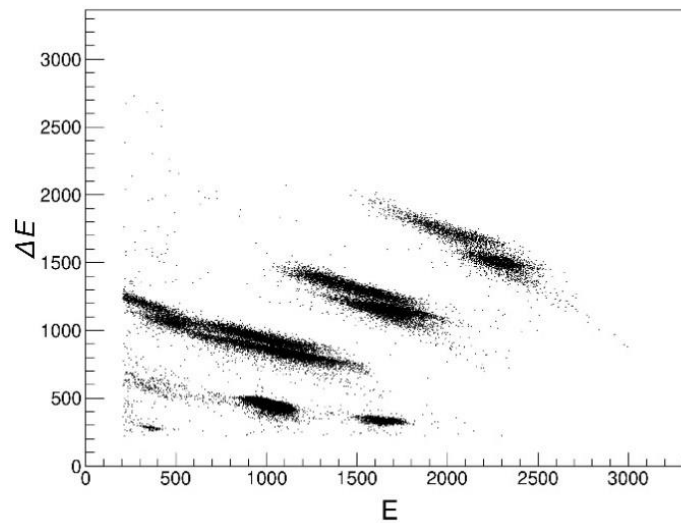
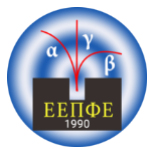


Figure 4. ΔE - E spectrum for $^8\text{B}+^{90}\text{Zr}$ at 40° degrees. The splitting of the bands due to the thickness of the DSSSD's strips can be observed. (see text).

SUMMARY

To summarize, we have collected elastic scattering and break-up data for the reaction $^8\text{B}+^{90}\text{Zr}$ at the sub-barrier energy 26.6 MeV at the *TriSol* facility of the University of Notre Dame. Data of elastic scattering for ^7Be were also analyzed for normalization purposes. The elastic scattering over Rutherford cross section ratios were extracted and compared with Optical Model and CDCC calculations. The obtained total reaction cross section either from OMP or the CDCC calculations, although in some disagreement between themselves, indicate larger magnitudes than the standard ones, obtained in systematics. Such large values are expected due to the small binding energy for this nucleus. As a first step in the analysis of the



breakup cross section, a detailed energy calibration for each strip of the detectors has been performed, taking into consideration the non-uniformity of the thickness of the detector. This is still in progress and it will be employed in the break-up analysis.

Acknowledgements

K. Palli acknowledges the support by the Hellenic Foundation for Research and Innovation (HFRI) under the 4th Call for HFRI Ph.D. Fellowships, Grant No. 009194.

References

- [1] N. Keeley et al., Prog. Part. Nucl. Phys. 59, 579 (2007)
- [2] N. Keeley et al., Prog. Part. Nucl. Phys. 63, 396 (2009)
- [3] L.F. Canto et al., Phys. Rep. 424, 1 (2006)
- [4] A. Di Pietro et al., Phys. Rev. Lett. 105, 022701 (2010)
- [5] G.R. Satchler, Phys. Rep. 199, 147 (1991)
- [6] B.B. Back et al. Rev. Mod. Phys. 86, 317 (2014)
- [7] J.J. Kolata et al. Eur. Phys J. A 52, 123 (2016)
- [8] C.L. Jiang et al., Phys. Rev. Lett. 89, 052701 (2002)
- [9] C.L. Jiang et al., Phys. Rev. C 81, 024611 (2010)
- [10] G. Montagnoli et al., Phys. Rev. C 85, 024607 (2012)
- [11] A. Pakou et al., Phys. Rev. C 102, 031601(R) (2020)
- [12] A. Pakou et al., Eur. Phys. J. A 51: 55 (2015)
- [13] L. Yang et al., Nat. Commun., 13, 7193 (2022)
- [14] M. Mazzocco et al., Phys. Rev. C, 100, 024602 (2019)
- [15] P. D. O'Malley et al., Nucl. Instrum. Methods Phys. Res. Sect A, 1047, 167784 (2023)
- [16] K. Palli et al., Phys. Rev. C, 107, 064613 (2023)
- [17] K. Palli et al., HNPS2022 Proceedings vol. 29, pp 52-57 (2023)
- [18] I.J. Thompson et al., Nucl. Phys. A 505, 84 (1989)
- [19] J. Raynal, Phys. Rev. C 23, 2571 (1981)